

# On the light-bending model of X-ray variability of MCG–6-30-15

Piotr T. ŻYCKI<sup>1</sup>, Ken EBISAWA<sup>2,3</sup>, Andrzej NIEDŹWIECKI<sup>4</sup> and Takehiro MIYAKAWA<sup>2,3</sup>

<sup>1</sup>*Nicolaus Copernicus Astronomical Center, Bartycka 18, Warsaw, Poland*  
*ptz@camk.edu.pl*

<sup>2</sup>*The Institute of Space and Astronautical Science, Japan Aerospace Exploration Agency, 3-1-1 Yoshinodai, Chuo, Sagami-hara, Kanagawa 229-5210, Japan*

<sup>3</sup>*Department of Astronomy, Graduate School of Science, University of Tokyo, 7-3-1 Hongo, Bunkyo-ku, Tokyo 113-0033, Japan*

<sup>4</sup>*University of Łódź, Department of Physics, Pomorska 149/153, 90-236 Łódź, Poland*

(Received 2010 March 6; accepted 2010 June 22)

## Abstract

We apply the light bending model of X-ray variability to *Suzaku* data of the Seyfert 1 galaxy MCG–6-30-15. We analyze the energy dependence of the root mean square (rms) variability, and discuss conditions necessary for the model to explain the characteristic decrease of the source variability around 5-8 keV. A model, where the X-ray source moves radially rather than vertically close to the disk surface, can indeed reproduce the reduced variability near the energy of the Fe  $K_{\alpha}$  line, although the formal fit quality is poor. The model then predicts the energy spectra, which can be compared to observational data. The spectra are strongly reflection dominated, and do *not* provide a good fit to *Suzaku* spectral data of the source. The inconsistency of this result with some previous claims can be traced to our using data in a broader energy band, where effects of warm absorber in the spectrum cannot be neglected.

**Key words:** galaxies:active – galaxies: individual (MCG-6-30-15) – X-rays:galaxies

## 1. Introduction

The Seyfert 1 galaxy MCG–6-30-15 shows the best example of a very broad Fe  $K_{\alpha}$  fluorescent line in its X-ray spectrum (Tanaka et al. 1995; see Reynolds & Nowak 2003 for review). According to numerous studies (e.g., Miniutti et al. 2007 and references therein) the line is produced well inside the marginally stable orbit for a Schwarzschild black hole, requiring a (maximally) rotating black hole. Uncertainties remain, though, as to the robustness of the broadness of the line, since the source has a very complex ionized absorber (e.g., Otani et al. 1996; Lee et al. 2001) and the details of the line modelling (e.g. its width) are rather sensitive to the description of the absorber (Miller, Turner & Reeves 2008; Miyakawa, Ebisawa & Inoue 2010).

At the same time, the variability properties of the line are rather incompatible with a simple geometrical ideas of the central accretion flow. The  $K_{\alpha}$  line, and the Compton reflection component associated with it appear to be much less variable than the continuum producing the reprocessed component. This was pointed out by Inoue & Matsumoto (2001, 2003), and later confirmed by many authors (e.g., Fabian et al. 2002). The line does not follow the continuum variability in a simple way, although some changes in the line profile/flux are observed (Iwasawa et al. 1996).

In simple geometrical scenarios the line and reflected continuum should respond to rapid variations of the primary continuum driving the reprocessed components. An explicit decomposition of the MCG–6-30-15 spectra onto components which can be interpreted as variable and constant one was done by Miller et al. (2008) using the

Principal Component Analysis method. The constant component appears to have a shape of a mildly ionized reflection, while the variable one corresponds to a broad-band continuum with ionized absorption.

A way of reconciling these two properties of the  $K_{\alpha}$  line was the so called “light bending model” (LBM) by Miniutti & Fabian (2004). The idea is that, for a source close to the central black hole, light bending and other relativistic effects will affect much more the observed primary emission than the reflected component. Thus, as the position of the source changes, the observed flux of the primary source will vary more than the flux of the reflected component. The model gained popularity despite it being rather ad hoc and having no obvious relation to the whole body of knowledge on X-ray variability of accreting black hole systems (see McHardy 2010 for a recent review and references).

The properties of the LBM were reanalyzed by Niedźwiecki & Życki (2008, hereafter NZ08), where it was concluded that in the original formulation the model actually failed to explain the data (see also Niedźwiecki & Miyakawa 2010, hereafter NM10). NZ08 suggested an alternative geometrical scenario, where the source moves radially (rather than vertically, as in the original formulation), very close to the disc surface. Then, light bending to the disc plane, an effect specific to the (extreme) Kerr metric causes the blue peak of the line to be approximately constant. The best variant of the model to explain the lack of variability of the line was that assuming the intrinsic source luminosity followed the Keplerian accretion disc emissivity (see fig. 7 in NZ08). Here, for radii  $\leq 3R_g$ , where  $R_g = GM/c^2$ , the line flux is almost constant, while

the primary source flux changes by a factor of  $\approx 7$ .

In the following paper NM10 extended the model calculations to include the reflected continuum. The full model was then applied the *Suzaku* rms( $E$ ) spectra of MCG–6–30–15. The rms( $E$ ) spectrum is defined as follows,

$$\text{rms}(E) = \frac{1}{\langle F(E) \rangle} \sqrt{\frac{\sum_i^N [F_i(E) - \langle F(E) \rangle]^2}{N-1}},$$

where the sum is over  $N$  contributions to flux  $F(E)$  at energy  $E$ , while  $\langle F(E) \rangle$  is the mean value of the flux. The rms( $E$ ) is thus a measure of the source variability, as a function of energy,  $E$ . The rms( $E$ ) spectra could indeed be modelled assuming that the source is located very close to the black hole,  $R = 1.6\text{--}3R_g$ . The rms( $E$ ) spectra computed assuming that spectra from 3–5 random radii within that range contribute to the emission could indeed match the shape of the observed rms( $E$ ). However, to match the amplitude of the rms( $E$ ) the intrinsic source normalization had to be assumed to vary. The intrinsic variability deprives the model its major attracting feature, namely the explanation of the constancy of the reflected component. On the other hand it may go some way towards explaining other key features of observed X-ray variability of Active Galactic Nuclei: the power spectrum, hard X-ray time lags, etc.

In this paper we investigate the model properties in some more detail. Our main purpose is to compute the energy spectra from the model and compare them with the *Suzaku* spectral data of MCG–6–30–15.

## 2. The light bending model

Our computations of the model are described in detail in NZ08 and NM10, following the original formulation by Miniutti & Fabian (2004). Here we give only a brief summary of its assumptions and properties. We assume a maximally rotating Kerr black hole and we consider the geometry, where the X-ray source moves radially, very close to the disk surface. The motion is along the line of constant polar angle,  $\theta$ , with  $H = 0.07R$ , where  $H$  is the height of the source. The intrinsic luminosity of the source follows the Keplerian accretion disk emissivity,  $L^{\text{PT}}(R)$ , (Page & Thorne 1974; model  $S^{\text{PT}}$  in NZ08), where

$$L^{\text{PT}}(R) = \frac{3GM\dot{M}}{8\pi R^3} R_R(r, a),$$

where  $r = R/R_g$ , and  $R_R(r, a)$  is the relativistic correction factor, containing the zero-inner torque condition and dependent on radial distance  $r$  and black hole angular momentum  $a$  [see Krolik 1999 for explicit form of  $R_R(r, a)$ ]

Then NZ08 show (see fig. 7 there) that, for  $R \leq 3R_g$  the observed flux of the Fe line is practically constant while the observed flux of the primary continuum varies by a factor of  $\approx 7$ . We illustrate this result in Fig. 1, which shows the model spectra for different radii  $\leq 3R_g$ . The flux of the reflected component (uniquely related to the flux of the Fe  $K_\alpha$  line for a given primary spectral shape and reflector ionization) is practically constant, while the

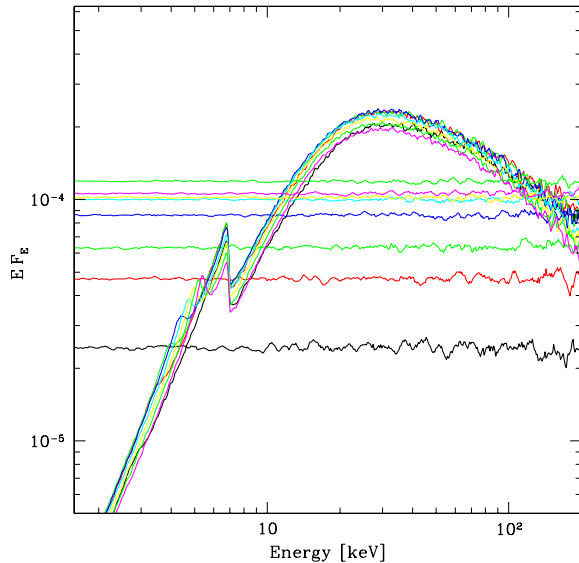


**Fig. 1.** The light bending model energy spectra from the  $S^{\text{PT}}$  model of NZ08, i.e. assuming that the intrinsic source luminosity follows the accretion disk dissipation rate (for  $a=0.998$ ) and the source can move along the line of constant polar coordinate with its height  $H = 0.07R$ . Observation (inclination) angle is  $i = 35^\circ$  and the source radial positions (corresponding to different curves) are 1.6, 1.8, 2, 2.2, 2.4, 2.6, 2.8,  $3R_g$ . The observed level of the direct source emission (represented by the approximately horizontal lines) depends then strongly on the source position, while the reflected component (and, in consequence the Fe line) is almost constant (see also fig. 7c in NZ08).

primary emission changes significantly. In the following computations we use the model in the version extended by NM10, where the radial location of the X-ray source is generated from a distribution  $P(r) \propto r^\delta$ , with  $\delta = -1.5$  (sources concentrated towards the black hole), and the intrinsic luminosity is randomized by being generated from a gaussian distribution centered at  $L^{\text{PT}}(R)$ , with standard deviation  $\sigma(R) = 0.2L^{\text{PT}}(R)$  (note that the randomization of luminosity is not included in the spectra plotted in Fig. 1).

We note here that the model predicts spectra which are strongly reflection dominated. This is a necessary consequence of the basic assumptions of the light bending model. The major problem then the model will face is whether such reflection dominated spectra can be compatible with MCG–6–30–15 data. We note that Fabian et al. (2002) did suggest that the X-ray spectra of Seyfert 1 galaxies may be reflection dominated but no fits to data of MCG–6–30–15 were presented. Since then, such reflection dominated spectra have been claimed to be good fits to data from a number of objects, including MCG–6–30–15. Most recent analysis of this source was published by Miniutti et al. (2007), where *Suzaku* data were analyzed. The large value of the amplitude of reflection inferred from the fits,  $\Omega/(2\pi) \approx 4$ , is claimed to be consistent with LBM.

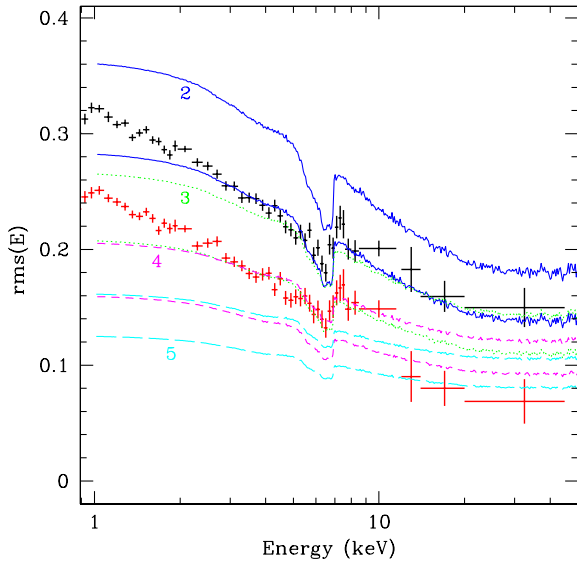


**Fig. 2.** The  $\text{rms}(E)$  dependence from Suzaku data of MCG-6-30-15, together with model curves. Data points show  $\text{rms}(E)$  for time bin of 16384 sec (upper set) and 131072 sec (lower set). Each pair of curves shows a  $\pm 1\sigma$  range of  $\text{rms}(E)$  from an ensemble of realizations of the model. Numeric labels show  $n_R$  – the number of radii contributing to each spectrum (see text, Sec 3, for details).

### 3. Modelling the energy dependence of the r.m.s

Results of NZ08 imply that a sequence of spectra from  $R \leq 3R_g$  will produce a  $\text{rms}(E)$  with a dip around the line energy, since the amplitude of reflected continuum is the same for all radii (Fig. 1).

Physically, we can expect that a spectrum from a given time interval of observation,  $T$ , will consist of contributions from a number of radii, the number depending on  $T$ . We treat the number of radii,  $n_R$ , as a parameter of the model, since the exact physical processes responsible for generating active regions are not known. The  $\text{rms}(E)$  spectrum is thus computed generating  $n_R$  values of radius from the  $1.6R_g \leq R \leq 3R_g$  range, adding energy spectra from these radii to form one basic spectrum, and then repeating the process  $N$  times, which corresponds simply to dividing the whole observation into  $N$  intervals. The  $\text{rms}(E)$  is computed from these  $N$  spectra.

A single  $\text{rms}(E)$  spectrum is just one realization of a random process. Repeating the above procedure would produce different  $\text{rms}(E)$ . To estimate the range of possible  $\text{rms}(E)$  behavior we repeat the procedure 1000 times, and plot the resulting  $\pm 1\sigma$  range of  $\text{rms}(E)$  in Fig. 2. Since we do not perform formal fitting ( $\chi^2$  minimization) of the model to the  $\text{rms}(E)$  data, the plot helps to estimate the optimum value of a parameter, in this case  $n_R$ . Specifically,  $\text{rms}(E)$  computed with  $n_R = 2-3$  gives the best match to the shorter time scale (16 ksec) observed  $\text{rms}(E)$ , while  $n_R = 4-5$  might be appropriate for the longer time scale  $\text{rms}(E)$ , although in the latter case

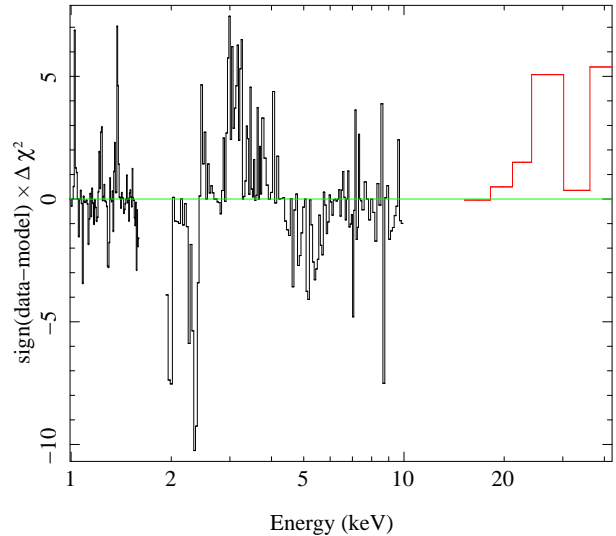


**Fig. 3.** Contributions to  $\chi^2$  from fitting the spectral model predicted by the LBM matching the  $\text{rms}(E)$  relation, to the time averaged Suzaku data of MCG-6-30-15. The fit is not satisfactory, with  $\chi^2_\nu \approx 1.5$ . The model spectrum is strongly reflection dominated and extremely relativistically smeared, since the source radial position  $R \leq 3R_g$ .

the slope of the model  $\text{rms}(E)$  is rather flatter than that of the data. The normalization of the model  $\text{rms}(E)$  spectrum is not adjusted to best match the data. This is different than the usual practice with energy spectral fitting, where the model amplitude is adjusted to give lowest possible  $\chi^2$ . Therefore the formal  $\chi^2$  values computed from these  $\text{rms}(E)$  models are rather high, the lowest values of  $\chi^2$  per data point being  $\approx 2$ .

### 4. Modelling the energy spectra

#### 4.1. Energy spectra predicted by the light bending model

We now present the energy spectra implied by the fits of the LBM to the  $\text{rms}(E)$  data and attempt to compare these with the spectral data of MCG-6-30-15.

Each realization of the  $\text{rms}(E)$  yields certain mixture of energy spectra from a number of radii, with relative weights resulting from the normalizations generated in the process (depending on the radius and the random amplitude around the  $L^{\text{PT}}(r)$  value). The total spectrum is then a sum of all these spectra. The spectra are strongly reflection dominated (Fig 1) with the amplitude of reflection,  $\Omega/(2\pi)$  reaching a factor of  $\approx 5$ .

We fit the January 2006 Suzaku XIS and PIN time averaged data in the range 1-40 keV. Importantly, in this energy range the effects of warm absorber cannot be neglected, so we fit a model which includes description of the absorber. Specifically, we apply a warm absorber model constructed from XSTAR calculations (Kallman et al. 2004). We find that a double model (low and high ionization) is necessary and sufficient to model the data (Sec 4.2; see also Miyakawa et al. 2009 for details of data reduction and warm absorber modelling).

We do preliminary fitting of the spectra from the NZ08 LBM model to the data. The source’s radial position is the most important fitting parameter. Computations of the reflected component were done only for cold plasma ( $\xi = 0$ ) and for Solar abundances of metals (constructing a grid of models is not practical due to computing resources required), therefore the model is not as general as other models available in XSPEC. The fits are generally poor, with reduced  $\chi^2_{\nu} = 1.8 - 1.9$ . Strongest  $\chi^2$  residuals appear below 5 keV.

We construct a more general reflection model by using the results of computations by Ross & Fabian (2005). Their model (table model `reflion` in XSPEC) includes all relevant atomic physics, including the Fe line emission (although it is not valid for low ionization,  $\xi < 30$ ). It was also used in many previous papers (e.g., Miniutti et al. 2007). We now apply relativistic effects by convolving the `reflion` spectrum with the transfer function from our LBM calculations for a given radius. Then, we add a power law continuum normalized so that the amplitude of the reflected component corresponds to that from the LBM computations. To achieve this, we use the ratio of the numbers of photons in the primary and reflected continua above 12 keV (the limit is important to exclude the effects of ionization). Finally, we sum the spectra over the set of radii. The resulting model is thus parameterized by primary power law slope,  $\Gamma$ , ionization parameter,  $\xi$ , Fe abundance and the inclination angle. The amplitude of reflection and relativistic smearing effects (i.e. the radial emissivity) result from the properties of the LBM and are thus fixed for a given set of radii.

This spectral model gives somewhat better fit, but it is still not satisfactory, with  $\chi^2_{\nu} \approx 1.5$  (Fig 3). Strong enhancement of reflection drives the primary continuum to be steep,  $\Gamma \approx 2.4$ , which seems incompatible with the slope required for the lower energy range (Fig 4) and, in consequence, significant deviations in  $\chi^2$  are present at  $E < 6$  keV. The best fits are obtained for inclination of  $40^\circ$  and Fe abundance equal to Solar. The quality of spectral fits is basically independent of the model realization, contrary to the quality of the  $\text{rms}(E)$  fits.

#### 4.2. Time averaged spectrum of MCG–6–30–15

According to some earlier studies, the reflection dominated spectra provide good description of the MCG–6–30–15 data, which fact has been used as a supporting argument for the applicability of the LBM. In particular, Miniutti et al. (2007; see also references therein) fitted the January 2006 Suzaku data with a model comprising cutoff power law continuum and ionized reflection (XSPEC `reflion` model of Ross & Fabian (2005) with relativistic smearing modelled with extreme Kerr metric transfer function of Laor (1991; XSPEC `kdblur2` model). Using this model Miniutti et al. obtain their best fit with strongly enhanced reflection,  $\Omega/(2\pi) \approx 4$ . The reflected component is strongly smeared, with inner disk radius of  $1.7 R_g$  and illumination emissivity following very steep,  $r^{-4.4}$ , dependence up to the break radius of  $6 R_g$ , beyond which the emissivity is flatter,  $r^{-2.5}$ .

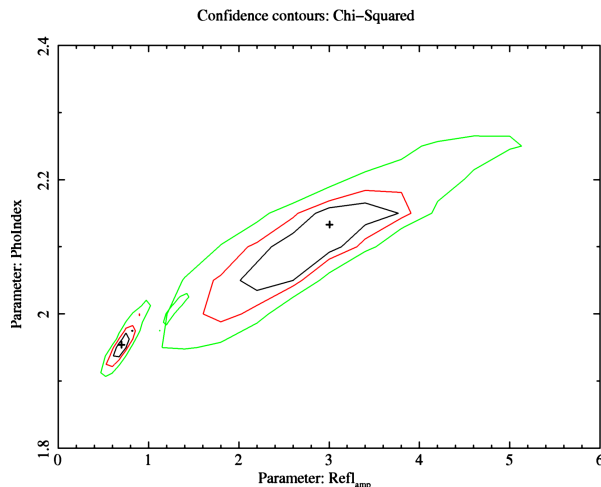


**Fig. 4.** The  $\chi^2$  contours in the  $\Omega/(2\pi)$ - $\Gamma$  plane for model fits to *Suzaku* data of MCG–6–30–15 in two cases: data above 3 keV, no warm absorber model (big contours) and data above 1 keV with a warm absorber model included (small contours). There is a clear and significant dependence of the amplitude of reflection on the data range/model components used.

In order to understand then why our results disagree with those earlier ones, we compare the results of fitting the same data with the same reflection model (i.e., the relativistically smeared `reflion` model) in two cases: (1) using only data above 3 keV, assuming that warm absorber does not affect the spectrum (as in Miniutti et al. 2007), and (2) using the data above 1 keV and attempting to describe the warm absorber. The warm absorber model, computed with XSTAR is prepared as a table model on a grid of  $20 \times 20$  values of column density,  $N_H$ , and ionization parameter,  $\xi$  (Miyakawa et al. 2009). We use two tables (lower and higher ionization), having checked that a single- $\xi$  model does not provide a good fit, while adding a third table does not improve the fit. We assume that the radial emissivity for line profile computation is the same as in Miniutti et al. (2007) and we keep it fixed, but we let the inner disk radius and inclination to be free. We keep the outer disk radius fixed at  $400 R_g$ . The Fe abundance is also free to fit, as is obviously the overall reflection amplitude.

We reproduce the results of Miniutti et al. (2007) in the first case, where only data above 3 keV are used. However, with broader energy band data the best-fit results are very different. The spectral index is smaller (harder spectrum) and the reflection amplitude is much smaller, in fact less than 1. In Fig. 4 we show the  $\chi^2$  contours in the spectral index – reflection amplitude plane, for both considered cases. The inner disk radius, characterizing the broadening of the line is comparable in both cases.

Our results mean that, to state it conservatively, the derived parameters of the reflection component are strongly model dependent. Fits in broader energy band yield harder spectrum and, in consequence, much smaller amplitude of reflection than fits performed in the  $E > 3$  keV energy band. This is a problem for LBM since it neces-



sarily predicts reflection dominated spectra.

It is not our goal here to construct more complex models and to study the dependence of the reflection parameters of the way how absorption is modelled. It seems that the solutions of Miller et al. (2008) and Miniutti et al. (2007) cover the whole broad range of possibilities. We simply want to emphasize that, in the context of our considerations, the support for the LBM depends on modelling the complex spectrum of MCG–6-30-15.

## 5. Discussion and conclusions

The light-bending model is an attempt to reconcile the extreme width of the Fe line with its lack of variability, first reported in MCG–6-30-15. It invokes extreme relativistic effects to explain weaker variability of the reprocessed spectral components compared to the primary components. Following the original formulation of the model by Miniutti & Fabian (2004) we reconsidered the model in greater details (NZ08, NM10) pointing out some inaccuracies in the original version. Reduced variability of the Fe line compared to primary continuum is indeed possible, but for a radially rather than vertically moving source.

Quantitatively, the model is able to reproduce the  $\text{rms}(E)$  relation, in particular the drop near the Fe line energy, but only if some intrinsic variability of the X-ray source is assumed (NM10). That is not necessarily a bad thing since it might go some way towards reproducing the usual characteristics of X-ray variability (e.g., power spectra), which the original model does not address. One possible test of the model is then to construct the energy spectra and compare these to the data. The model spectra are obviously strongly reflection-dominated and relativistically smeared.

We find that the reflection-dominated spectra do not fit the data, contrary to previous studies (Miniutti et al. 2007 and references therein). There is a significant dependence of the best-fit models on the energy range of the fitted data. The effects of warm absorber in the spectrum are not limited to below 3 keV, and so using the data below this energy and including a warm absorber model gives very different results compared to fits without the warm absorber and data above 3 keV. In this respect our results can be located between the results of Miller et al. (2008) and Miniutti et al. (2007), which can be thought of as absorption-dominated and reflection-dominated solutions, respectively. We note that the dependence of reflection parameters on details of the warm absorber description applies also to the width of the Fe  $K_{\alpha}$  line. While this is usually claimed to be extremely broad, data modelling including complex warm absorber models (Miller et al. 2008; Miyakawa et al. 2010) yields good descriptions of the broad band data of MCG–6-30-15 without extremely broad Fe line.

MCG–6-30-15 is not the only source showing certain degeneracy between reflection and absorption in their X-ray spectra. Similar situation occurs in the X-ray binary XTE J1650-500 where Miniutti, Fabian & Miller (2004) presented fits of models with extremely broad Fe

line, while Gierliński & Done (2006) demonstrated that the Fe line does not need to be so broad, if complex absorption and reflection models are applied. Another spectral feature where this kind of ambiguity is observed are the so called soft X-ray excesses observed in many Active Galactic Nuclei. These can be modelled equally well by absorption and reflection effects (Sobolewska & Done 2007). The situation may appear somewhat frustrating, appearing despite years of data collecting and efforts to understand them. More importantly though, the implications of the two models are very different and far-reaching, since they touch the base of our interest in X-ray astronomy. Studying effects of extreme gravity near compact objects was and still is one the main driving forces for developing technologies for X-ray observations.

Summarizing, we fit the spectra predicted by the LBM of NZ08 to Suzaku data of MCG–6-30-15 and find that the model does *not* fit the data, if the fits use data in the energy range where warm absorber effects are important. Detailed results depend on models of warm absorber, with more complex warm absorber models implying less extreme reflection.

## Acknowledgments

This work was partly supported by Japan Society for the Promotion of Science fellowship to PTZ. PTZ thanks ISAS/JAXA for their kind hospitality in March 2009. Partial support for this work came also from the Polish Ministry of Science and Higher Education through grant no. N203 011 32/1518.

## References

- Fabian A. C. et al., 2002, MNRAS, 335, L1
- Gierliński M., Done C., 2006, MNRAS, 367, 659
- Inoue H., Matsumoto Ch., 2001, AdSpR, 28, 445
- Inoue H., Matsumoto Ch., 2003, PASJ, 55, 625
- Iwasawa K. et al., 1996, MNRAS, 282, 1038
- Kallman T. R., Palmeri P., Bautista M. A., Mendoza C., Krolik J., 2004, ApJS, 155, 675
- Krolik J. H., 1999, Active Galactic Nuclei (Princeton University Press, Princeton)
- Laor A., 1991, ApJ, 376, 90
- Lee J. C., Ogle P. M., Canizares C. R., Marshall H. L., Schulz N. S., Morales R., Fabian A. C., Iwasawa K., 2001, ApJ, 554, L13
- M<sup>c</sup>Hardy I., 2010, in The Jet Paradigm, Lecture Notes in Physics, Volume 794. (Springer-Verlag Berlin Heidelberg), p. 203
- Miller L., Turner T. J., Reeves J., 2008, A&A, 483, 437
- Miniutti G., Fabian A. C., 2004, MNRAS, 349, 1435
- Miniutti G., Fabian A. C., Miller J., 2004, MNRAS, 351, 466
- Miniutti G. et al., 2007, PASJ, 59, 315
- Miyakawa T., Ebisawa K., Terashima Y., Tsuchihashi F., Inoue H., Życki P. T., 2009, PASJ, 61, 1355
- Miyakawa T., Ebisawa K., Inoue H., 2010, PASJ, in press
- Niedźwiecki A., Życki P. T., 2008, MNRAS, 386, 759 (NZ08)
- Niedźwiecki A., Miyakawa T., 2010, A&A, 509, 22 (NM10)
- Otani C. et al., 1996, PASJ, 48, 211
- Page, D. N., Thorne, K. S., 1974, ApJ, 191, 499

- Reynolds C. S., Nowak M. A., 2003, *Phys Rep*, 377, 389  
Ross R., Fabian, A. C., 2005, *MNRAS*, 358, 211  
Sobolewska M., Done C., 2007, *MNRAS*, 374, 150  
Tanaka Y., et al., 1995, *Nature*, 375, 659